

Naresh Kumar Sethy\*, Zeenat Arif, Pradeep Kumar Mishra and Pradeep Kumar

# Green synthesis of TiO<sub>2</sub> nanoparticles from *Syzygium cumini* extract for photo-catalytic removal of lead (Pb) in explosive industrial wastewater

<https://doi.org/10.1515/gps-2020-0018>

Received August 20, 2019; accepted December 09, 2019.

**Abstract:** Green synthesis is a simple, non-toxic, economical and eco-friendly approach for the synthesis of nanoparticles. In the present work, nanoparticles of titanium dioxide (TiO<sub>2</sub> NPs) were synthesized using an aqueous solution of *Syzygium cumini* leaf extract as a capping agent. These green synthesized TiO<sub>2</sub> NPs were further evaluated for photo catalytic removal of lead from industrial wastewater. Obtained nanoparticles were characterized using: high-resolution scanning electron microscopy (HRSEM), high-resolution transmission electron microscopy (HRTEM), X-ray energy dispersive spectroscopy (EDS), Fourier transform infrared (FT-IR) spectroscopy, X-ray diffraction (XRD), dynamic light scattering (DLS) and Brunauer-Emmett-Teller (BET). Obtained results revealed that synthesized TiO<sub>2</sub> NPs possess spherical morphology with anatase phase with a large BET surface area of 105 m<sup>2</sup>/g. Photo catalytic studies of TiO<sub>2</sub> NPs for lead removal from explosive wastewater were performed in a self-designed reactor. Inductive coupled plasma spectroscopy (ICP) was used to determine the lead concentration. Obtained results witnessed 75.5% removal in chemical oxygen demand (COD) and 82.53% removal in lead (Pb<sup>2+</sup>). This application of green TiO<sub>2</sub> NPs is being explored for the first time.

**Keywords:** green synthesis; *Syzygium cumini* extract; TiO<sub>2</sub> nanoparticles; photo-catalytic degradation; wastewater treatment

## 1 Introduction

Environmental safety is nowadays a prime global challenge. In this, water pollution is one of the alarming areas. Various types of discharges like heavy metals, dyes, and pesticides enters different water bodies turns out to be critical sources of water pollution. Among these, heavy metals are hazardous due to their high aquatic solubility and easy access to living body through the food chain causing various health disorders [1-7]. Among the heavy metals, lead (Pb) is a priority pollutant and is widely present [3]. Electroplating, mining, metal finishing, and lead smelting are some of the sources from which lead enters the water bodies [8]. As per the World Health Organization (WHO) and Environmental Protection Agency the maximum permissible limit of lead in the drinking water is 0.05 ppm [9,10]. So, it is of prime importance to restrict the lead concentration to the range 0.05-0.10 ppm before discharge to local water bodies [10,11]. Many research activities are being conducted to curb this environmental problem.

Conventional approaches like physical, chemical and biological processes are being followed for waste water treatment [12]. Each of these processes depends on factors like feasibility, efficiency, and economics [13]. Photo catalysis is a kind of chemical method which is in demand due to its simplicity, low cost, non-toxic, high degradation efficiency and excellent stability. In the process of photo catalysis, oxidation is induced by UV light and sensitized by photo catalysts such as TiO<sub>2</sub>, ZnO, etc. [14]. Among these, TiO<sub>2</sub> with band gap energy of 3-3.5 eV promotes the photo catalytic behavior in a considerable way [15]. The electron transfer mechanism in TiO<sub>2</sub> from valance band to conduction band during exposure to UV or visible light generates a hole (h<sup>+</sup>), which further contacts with water to form an OH radical. This OH radical will act as a strong oxidizing agent and stands responsible for removing organic pollutants, pesticides and heavy metals like lead (Pb) [16] from the waste water through photo oxidation mechanism.

\* Corresponding author: Naresh Kumar Sethy, Department of Chemical Engineering and Technology, Indian Institute of Technology (BHU), Varanasi-221005, India, e-mail: nareshks.rs.che15@itbhu.ac.in

Zeenat Arif, Pradeep Kumar Mishra and Pradeep Kumar, Department of Chemical Engineering and Technology, Indian Institute of Technology (BHU), Varanasi-221005, India






The generation electron, photon, and OH radical are written in the reactions shown below.



Nanoparticle synthesis through chemical route generally stands expensive due to the use of synthetic chemicals which are detrimental to the living eco

system [17]. On the other hand, synthesis through green route is a simple, less toxic, economical and eco-friendly way to synthesize nanoparticles from various extracts of plants, microbes, enzymes, etc. [18]. Few works on green synthesized nanoparticles and their usage in wastewater treatment are reported [19]. Literature on synthesis of TiO<sub>2</sub> NPs using various plant extract like *Glycosmis cochinchinensis* [20], *Jatropha curcas* [21], *Moringa oleifera* [22], *Aloe barbadensis* Miller [23], and *Psidium guajava* [24] is tabulated (Table 1).

**Table 1:** Nanoparticle synthesise from different plant extract.

SL. No.	Plant used for synthesis of TiO <sub>2</sub> NPs	Plant image	Particle size (nm)	Reference
1	<i>Glycosmis cochinchinensis</i>		35-45	[20]
2	<i>Jatropha curcas</i>		75	[21]
3	<i>Moringa oleifera</i>		12.22	[22]
4	<i>Aloe barbadensis</i> Miller		20	[23]
5	<i>Psidium guajava</i>		32.58	[24]

In this paper, titanium dioxide nanoparticles were synthesized from *Syzygium cumini* leaf extract using a green synthesis approach. Previously, *Syzygium cumini* extract was used for the synthesis of nanoparticles like iron, silver and gold but TiO<sub>2</sub> NPs was synthesized by using its leaf extract was a new one. Synthesized NPs were used to remove the lead contamination from explosive waste waters by photo catalytic degradation method. Experimental methodology, characterizations and obtained results were elaborately discussed in the following sections. This is first of its kind work to use green synthesized titanium dioxide nanoparticles as a catalyst for photo catalytic degradation of lead from industrial waste waters.

## 2 Experimental

### 2.1 Materials

Titanium-isopropoxide as purchased (TTIP Sigma-Aldrich, AR grade, purity > 97%) was used for the synthesis of TiO<sub>2</sub> nanoparticles. Fresh leaves of *Syzygium cumini* were collected from IIT (BHU) Varanasi campus and were further processed for use as bio-template. Industrial waste water having lead was collected from a commercial explosive manufacturing industry, Jharkhand, India. It was used directly without any purification and stored in a glass bottle and kept in the refrigerator for use.

### 2.2 Green synthesis of TiO<sub>2</sub> NPs

At first *Syzygium cumini* leaves, collected from the campus, were thoroughly washed with double distilled water to remove any dirt adhered to the surface. Now leaves were allowed to dry at 60°C temperature in a tray drier. Later, these dry leaves were subjected to comminution using laboratory grinder and obtained powder was collected and stored. Leaf extract, to be used as capping/stabilizing agent was prepared by mixing 20 g of powder with 100 mL of distilled water and heating the mixture at 80°C for 60 min. Extract obtained after heating was filtered using Whatman filter paper and was used as a capping/stabilizing agent for the synthesis of nanoparticles. TiO<sub>2</sub> NPs by the green route were prepared by adding 80 mL of 5 mM TTIP solution to 80 mL of *Syzygium cumini* extract in the ratio of 1:1 (volume/volume) followed by continuous stirring at room temperature for 8 h. The mechanism

behind the formation of TiO<sub>2</sub> NPs was hydrolysis of TTIP, which was the dominant pathway for the formation of TiO<sub>2</sub> NPs [25]. The leaf extract present in solution mixture act as a capping/stabilizing agent was to prevent agglomeration and achieving the desired shape and size of the TiO<sub>2</sub> NPs. After stirring the mixture was centrifuged at 9000 rpm for 10 min to separate the nanoparticles. Obtained wet powdered TiO<sub>2</sub> NPs were dried at 100°C for one night and then subjected to calcination at 570°C in a muffle furnace for 3 h. Thus, obtained TiO<sub>2</sub> NPs were collected and stored for further characterization and photo catalytic degradation of waste water was studied. Pictographic representation of the overall synthesis process is shown in Figure 1.

### 2.3 Characterization

Nanoparticles were characterized for physical, chemical, structural and morphological evaluations. Morphological evaluation of green synthesized TiO<sub>2</sub> nanoparticle was done by high-resolution scanning electron microscopy (HRSEM) (Nova Nano SEM 450) equipped with an energy dispersive X-ray spectroscopy system (EDAX Inc.). Chemical evaluation was done using Nicolet 560FT-IR spectroscopy in the range of 400-4000 cm<sup>-1</sup>. Physical evaluation was done using dynamic light scattering (DLS) (Nano plus common) to get particle size distribution, also stability of the nanoparticles as dispersion was analyzed using zeta potential analyzer (Malvern Instruments) and Brunauer-Emmett-Teller surface area analyzer (ASAP 2020, Micromeritics) was used to determine the surface area, pore size distribution and volume of pores. Structural evaluation of nanoparticles was performed using Ultima IV, Rigaku X-ray diffractometer (Cu-K $\alpha$  $\lambda$  = 0.154 nm) at a radiation of 40 kV/15 mA within the 2 $\theta$  range of 10°-80° at room temperature. Further the energy band gap of titanium dioxide nanoparticles was calculated using CARY-100 Bio UV-Visible spectrophotometer. Under the photo catalytic application of nanoparticles, the toxicity of the wastewater before and after photo catalytic oxidation is measured using inductive coupled plasma spectroscopy (Thermo Scientific).

### 2.4 Photo catalytic properties

The photo catalytic performance of the green synthesized TiO<sub>2</sub> nanoparticle from *Syzygium cumini* extract is studied on the explosive industrial wastewater source having lead contaminant. The wastewater samples were

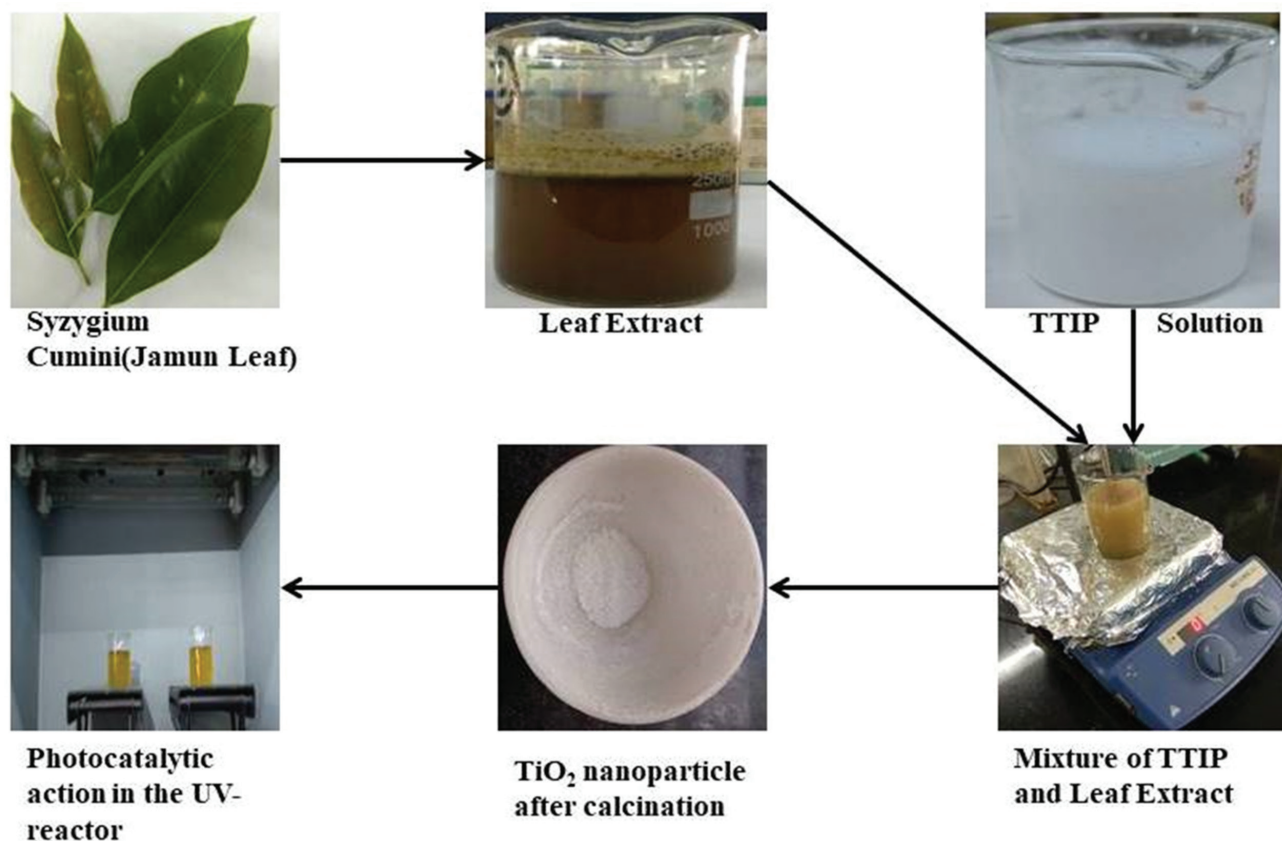


**Figure 1:** Synthesis of TiO<sub>2</sub> nanoparticle from *Syzygium cumini* leaf extract.

collected and stored at 6–7°C for further physicochemical analysis. Collected sample (500 mL) without altering the pH was treated photocatalytically using the green TiO<sub>2</sub> NPs (0.3 g) for 12 h in a self-designed and fabricated photocatalytic reactor. The reactor consists of three UV lamps of 15 W each. Initially, to establish the equilibrium between lead and TiO<sub>2</sub> nanoparticles the sample was kept in the dark (without UV) for 30 min. Afterward the lamps were switched on, and the samples were collected from the UV reactor at a regular interval of time and were centrifuged at 9000 rpm for 10 min to obtain a clear supernatant of industrial wastewater which was stored in sample bottles.

The lead concentrations were analyzed by inductive coupled plasma spectroscopy (Thermo Scientific). The operating conditions of the ICP instrument before analysis was set to camera temperature: –45.65, optics temperature: 38°C, pump rate = 45 rpm, gas flow rate = 1.5 L/min (argon) and wave length ( $\lambda$ ) = 220.353 nm. Standards taken for calibration plot were 1.25 ppm, 2.5 ppm, 5 ppm, and 10 ppm. A control sample without nanoparticle was also taken as a reference for the photocatalytic degradation study. For a comparative study, another experiment was done in the dark with TiO<sub>2</sub>

nanoparticles in the sample and sample were collected at a regular interval for analysis.

Chemical oxygen demand (COD) parameter was also monitored to determine the pollution profile by evaluating the removal efficiency of heavy metal ions and COD. COD analysis in the current work was done using UNIPHOS-COD analyser based on the principle of absorption of light at wavelength 595 nm by potassium dichromate in the digested sample.

### 3 Results and discussion

#### 3.1 X-ray diffraction (XRD)

XRD pattern of synthesized TiO<sub>2</sub> NPs as shown in Figure 2 indicates its crystalline nature. Significant peaks in a  $2\theta$  range of  $10^\circ < 2\theta < 80^\circ$  were observed at 25.38°, 37.97°, 48.14°, 54.40° and 62.71° and suitably matches to the Miller indices (hkl) values: (1 0 1), (0 0 4), (2 0 0), (1 0 5) and (2 0 4), respectively, to confirm the anatase phase. Obtained results were justified with JCPDS (Joint Committee on Powder Diffraction Standards) Card No.

78-2486 [26]. Weak peak at 30.98° was also observed and was assumed due to the orthorhombic crystalline structure. High crystalline nature of the NPs which was indicated by a sharp peak, favors the photo catalytic activity. Debye Scherrer's equation (Eq. 4) was used to calculate crystalline size of the particle.

$$d = 0.89\lambda/\beta \cos \theta \quad (4)$$

where  $d$  was the crystalline size of NPs,  $\lambda$  was the wavelength of the X-ray radiation source,  $0.89$  was a constant crystalline shape factor,  $\theta$  was the Bragg's diffraction angle, and  $\beta$  was the full angular width at half maximum (FWHM) of XRD peaks recorded at diffraction

angle  $2\theta$ . The average crystalline size of the green synthesized TiO<sub>2</sub> NPs was found to be 10 nm.

### 3.2 Dynamic light scattering (DLS) and zeta potential analysis

To analyze the particle size distribution, green synthesized TiO<sub>2</sub> NPs were subjected to dynamic light scattering (DLS) analysis. Here material was dispersed completely in distilled water using ultra-sonicator for DLS analysis. Results obtained as shown in Figure 3a, reveals the mono-disperse nature of particles with an average particle size was around 22 nm.

Nanoparticle stability was evaluated in term of zeta potential as shown in Figure 3b. It was found that the zeta potential value was strongly negative i.e.  $-18.7$  mV which implies good colloidal nature of particle which was fairly stable [27].

### 3.3 BET and FTIR analysis

The surface area analysis of synthesized nanoparticles was done using Brunauer-Emmett-Teller (BET) surface area analyzer. Other outputs like, pore size and pore volume were also obtained using Barrett-Joyner-Halenda analysis. Results revealed that synthesized TiO<sub>2</sub> NPs had high surface area of 105 m<sup>2</sup>g<sup>-1</sup> with 10.50 nm pore size and 0.278 cm<sup>3</sup>/g pore volume which will stand beneficial for photo catalytic action to treat the lead contaminated industrial wastewater. The obtained

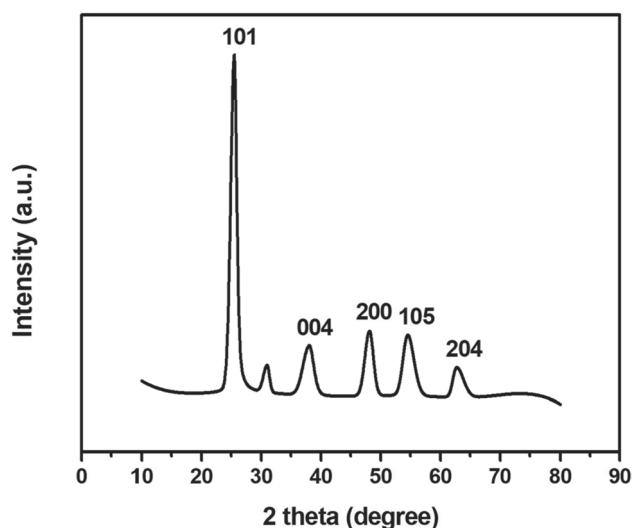


Figure 2: XRD pattern of synthesized TiO<sub>2</sub> nanoparticles.

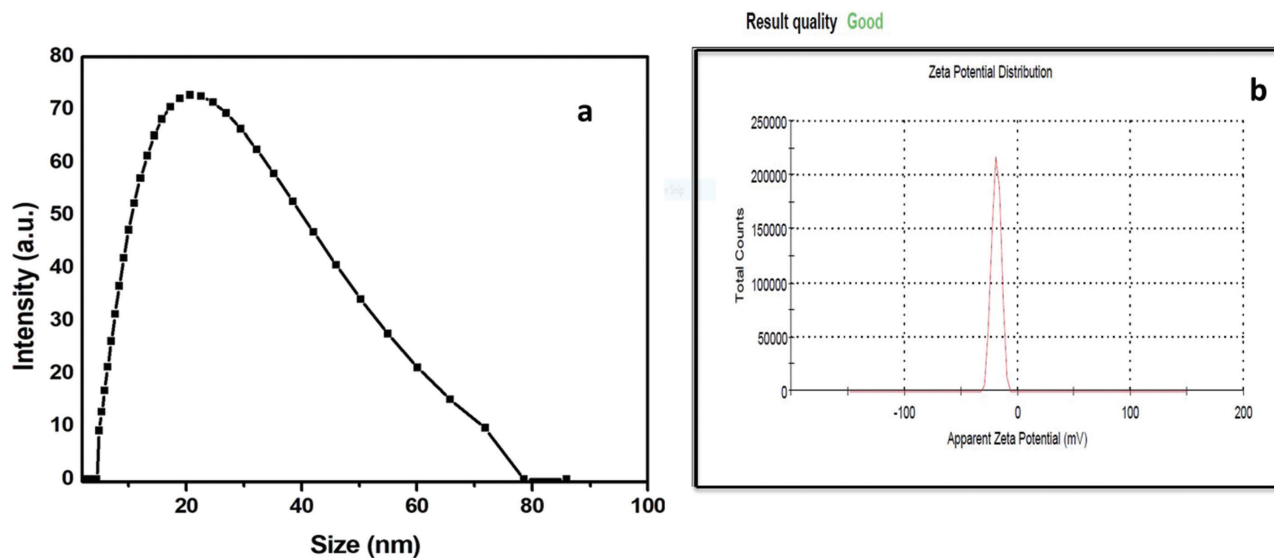


Figure 3: (a) Particle size distribution of synthesized TiO<sub>2</sub> nanoparticles; (b) Zeta potential analysis.

adsorption-desorption isotherms curve of the synthesized nanoparticle was shown in Figure 4a.

The FTIR spectra of green synthesized TiO<sub>2</sub> NPs were used to determine different functional groups responsible for the formation of nanoparticles. Figure 4b reveals that the green synthesized TiO<sub>2</sub> NPs had a large peak at 3354 cm<sup>-1</sup>, and a small peak at 1628 cm<sup>-1</sup> due to hydroxyl group and surface adsorbed water respectively [28]. This hydroxyl group was assumed to be responsible for the photo catalytic activity of NPs. FTIR spectrum of green synthesized nanoparticles also showed characteristic bands at 1024 cm<sup>-1</sup> which indicates the presence of C–O stretching alcohols, carboxylic acids, esters, and ethers. Peaks at 1024 and 493 cm<sup>-1</sup> were attributed to Ti–O stretching and Ti–O–Ti bridging stretching mode [29,30]. The peak at 493 cm<sup>-1</sup>

confirmed the presence of TiO<sub>2</sub> nanoparticles. No peak is observed at 2900 cm<sup>-1</sup> for C–H stretching which confirms that removal of the organic compound after calcination for 3 h at 570°C [31].

### 3.4 SEM-EDAX

The morphology of TiO<sub>2</sub> nanoparticles was determined by using HRSEM analysis. Obtained results as showcased in Figure 5a, reveals that the synthesized TiO<sub>2</sub> particles were in spherical in shape and aggregated into an irregular structure with an average diameter of 18 nm. It is observed that the powder particles were slightly agglomerated. Compositional analysis of synthesized TiO<sub>2</sub> nanoparticle was done by EDAX analysis. As shown in Figure 5b, wt%

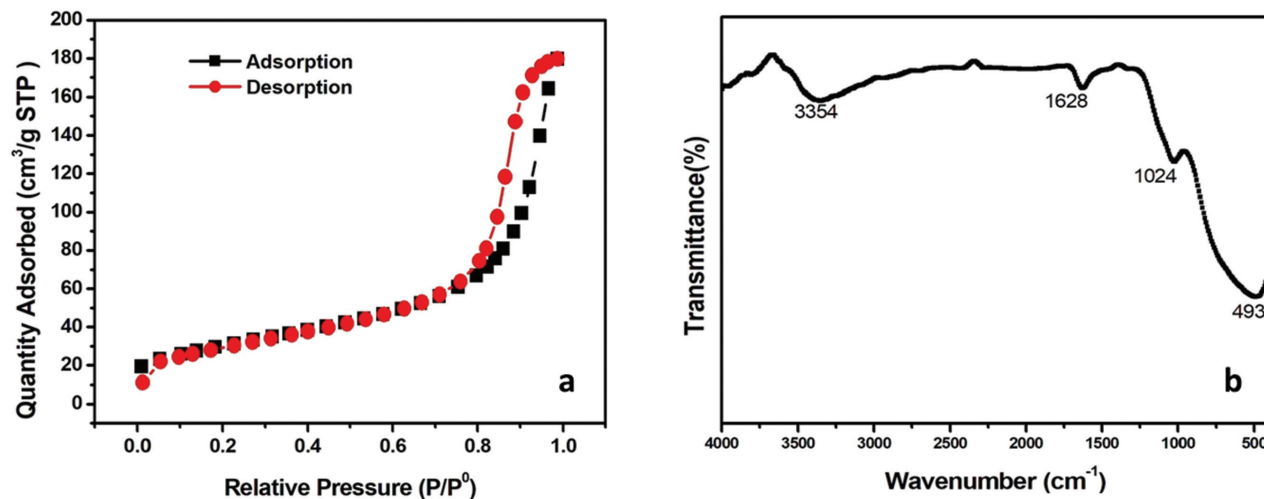


Figure 4: (a) Adsorption- desorption isotherms curve of the synthesized nanoparticle; (b) FTIR plot of synthesized TiO<sub>2</sub> NPs.

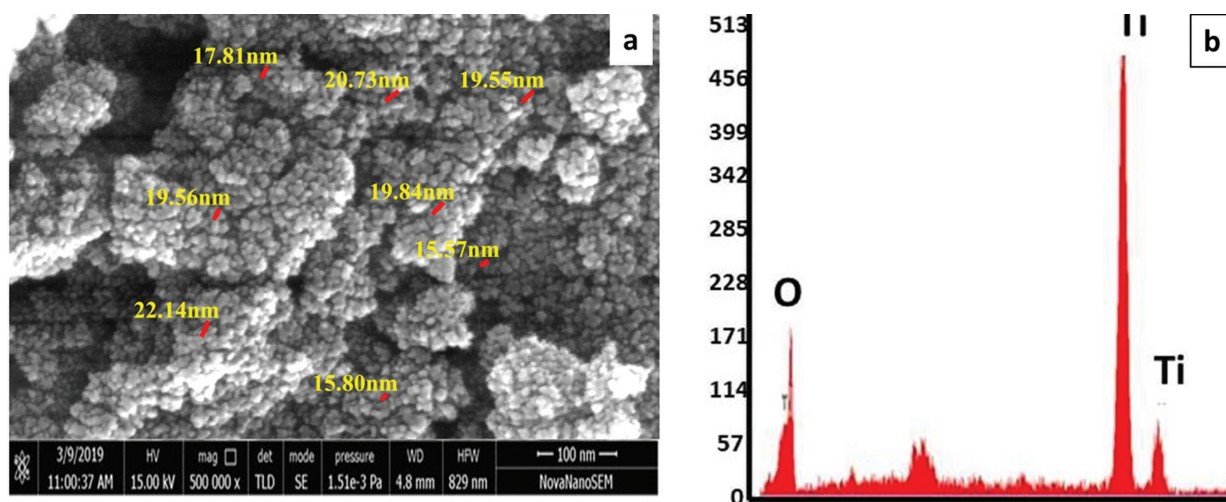


Figure 5: SEM-EDX image of synthesized TiO<sub>2</sub> NPs.

of Ti was found highest at 66.54%, and of oxygen (O) was at 33.46% and no other peaks are observed. This confirms the presence of TiO<sub>2</sub> particles.

### 3.5 TEM analysis

Figures 6a and 6b give the TEM image and SAED pattern of TiO<sub>2</sub> nanoparticles synthesized by green route. The average size of the particle in Figure 6a was found to be 11 nm which was near about to the crystal size calculated by Debye Scherrer's equation in the XRD result. On SAED image, the diffraction rings match with the XRD pattern and confirmed the crystallinity and anatase phase of the TiO<sub>2</sub> nanoparticles in Figure 6b [32].

### 3.6 UV-Vis spectroscopy of TiO<sub>2</sub> NPs

UV-Visible spectrophotometer was used to study the band gap of synthesized TiO<sub>2</sub> nanoparticles by green route. Results obtained as shown in Figure 7 showcase a prominent peak at 356 nm with absorbance less than 1. Strong peak at 356 nm in the range of 200 to 600 nm confirms the synthesis of greenTiO<sub>2</sub> NPs [33].

Energy band gap of synthesized TiO<sub>2</sub> nanoparticles by green route can be estimated using Eq. 5:

$$E_g = \frac{hc}{\lambda} \quad (5)$$

where  $E_g$  – band gap energy (eV),  $h$  – Planck's constant,  $c$  – light velocity (m/s), and  $\lambda$  – wavelength at maximum absorbance (nm).

From Eq. 5, the band gap energy ( $E_g$ ) to be calculated as 3.48 eV. UV absorbance spectra of TiO<sub>2</sub> conclude that it acts as a photo catalyst and reacts intensively in the presence of UV light due to the formation of OH radicals which responsible for removal of lead ions [34].

### 3.7 Photocatalytic activity

The performance of synthesized nanoparticles was tested for the photo catalytic treatment of lead-contaminated explosive industrial wastewater. The physicochemical properties of waste water before and after treatment were presented in the Table 2.

The degradation of wastewater was analysed by measuring the concentration of Pb as a function of time. At the same time, it was also significant to carry out a blank test (without NPs) to ascertain that degradation was mainly due to the photo catalytic reaction of TiO<sub>2</sub> NPs. Post treatment, the effectiveness of the treatment process was evaluated by calculating the removal efficiency using as per Eq. 6.

$$R (\%) = \frac{Pb_0 - Pb_t}{Pb_0} \times 100 \quad (6)$$

where  $Pb_0$  and  $Pb_t$  were the initial and final concentration of lead in wastewater before and after the photo catalytic treatment.

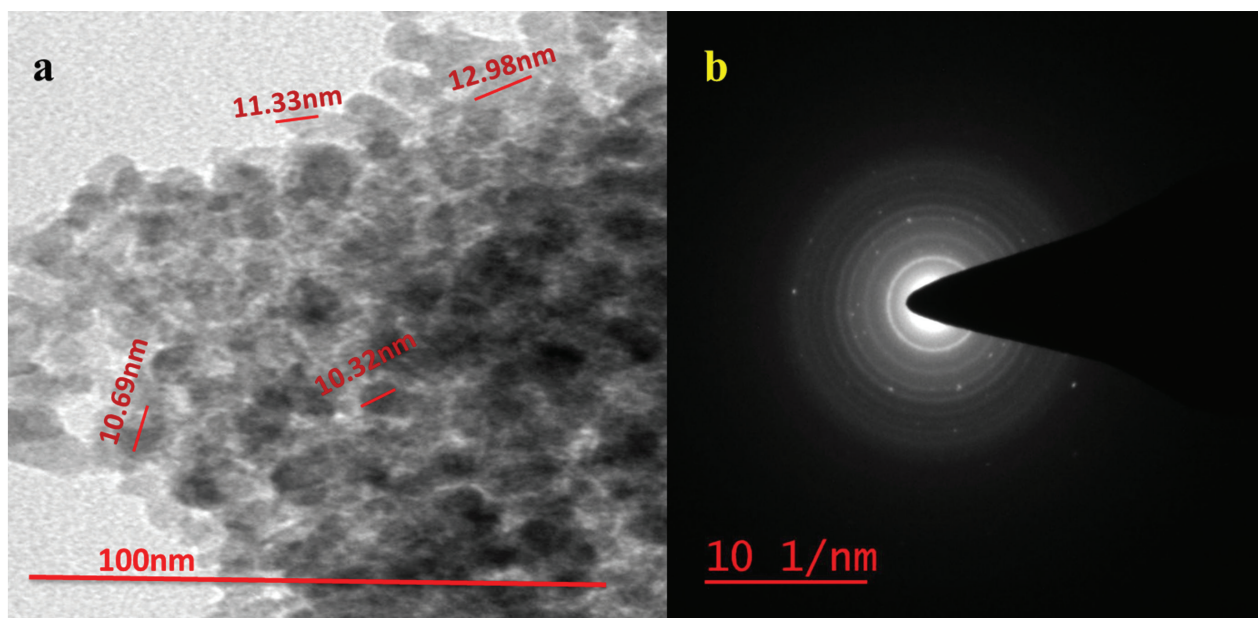


Figure 6: TEM analysis.

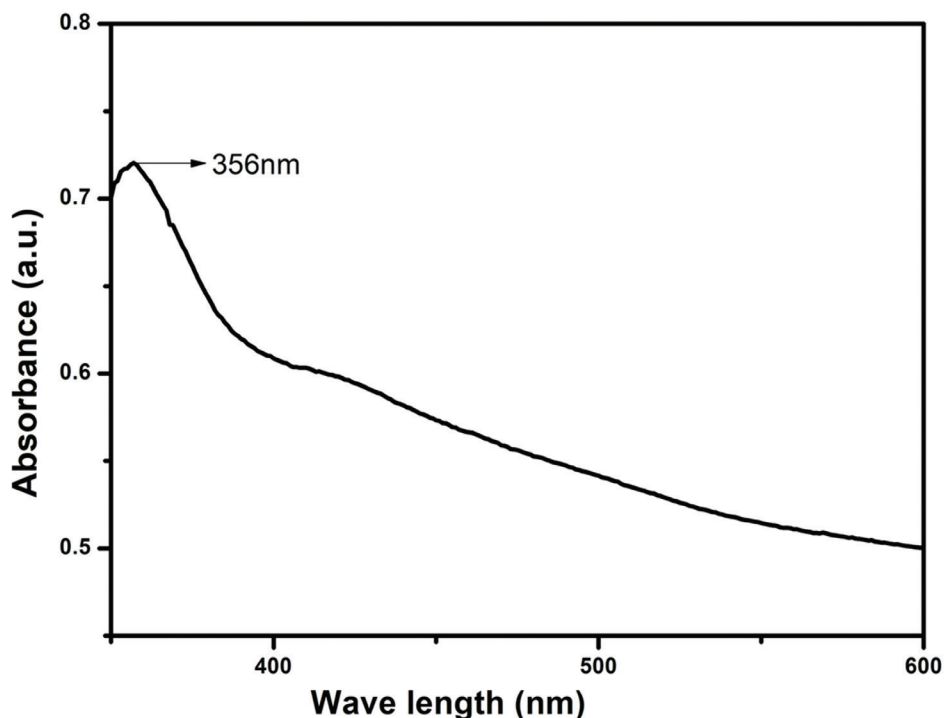


Figure 7: UV-Vis spectra of synthesized TiO<sub>2</sub> NPs.

Table 2: Water characteristics before and after treatment.

Physico-chemical parameter	Before treatment	After treatment
pH	7.6	7.8
Lead (ppm)	8.621	1.5
COD (mg/L)	8450	2004
Color (a.u.)	Yellow (0.15)	Light yellow (0.07)

The obtained values from the ICP analysis of lead concentration in the sample were given in Table 3.

Results after 17 h treatment showed a sharp decrease in Pb concentration from 8.6 ppm to 1.5 ppm in the presence of TiO<sub>2</sub> + UV when compared to experiments carried in dark condition where the concentration decreased to 8.35 ppm. This sharp decline in concentration was attributed to the photo-catalytic activity of TiO<sub>2</sub> NPs on lead ion present in the water sample, whereas in dark condition the minor change in concentration was attributed to the adsorption of Pb on TiO<sub>2</sub> surface [35]. The decrease in Pb concentration in the photolysis condition (only UV light) was due to photo degradation of Pb by the strong UV wavelength. Comparative results as shown in Figure 8a for uncatalyzed and TiO<sub>2</sub>-catalyzed degradation with time (12 h) reveals that the degradation rate is about 82.53% in TiO<sub>2</sub>-catalyzed, and only 3.14% in uncatalyzed.

This not only supports but also proves the role of TiO<sub>2</sub> NPs in the photo catalytic degradation of Pb.

Effect of Pb concentration on the photo catalytic degradation rate was also investigated and presented in Figure 8a. First-order law kinetic model as shown in Eq. 7 was used to analyse the photo catalytic degradation of Pb [36]:

$$r_{pb} = -dC_{pb}/dt = k_{app} C_{pb} \quad (7)$$

Equation 7 after integrating can be rewritten as:

$$\ln(C_{pbo}/C_{pb}) = k_{app} t \quad (8)$$

where  $C_{pbo}$  and  $C_{pb}$  are initial and final concentration of Pb (ppm),  $k_{app}$  represent the pseudo first-order constant (h<sup>-1</sup>), and  $t$  the time (h).

Graph between  $\ln(C_{pbo}/C_{pb})$  versus time ( $t$ ) for Pb was observed to be linear Figure 8b with a rate constant 0.097 h<sup>-1</sup>. R<sup>2</sup> value being greater than 0.96 indicates a good correlation with the first order kinetics. The large surface area of TiO<sub>2</sub> NPs provides a large number of active site which is responsible for the effective degradation.

Chemical oxygen demand (COD) of the original sample was 8450 mg/L, which was greater than the permissible limit. Water bodies with high loading of COD disturb the ecological functions which lead to adverse

Table 3: ICP and COD values at different condition.

Time (h)	Pb concentration (ppm) in absence of TiO <sub>2</sub> NPs + UV	Pb concentration (ppm) in presence of TiO <sub>2</sub> NPs + dark	Pb concentration (ppm) in presence of TiO <sub>2</sub> NPs + UV	COD (mg/L) in presence of TiO <sub>2</sub> NPs + UV
0	8.621	8.621	8.621	8450
2	8.621	8.560	7.844	6300
4	8.598	8.412	7.397	5500
6	8.598	8.35	5.325	4900
8	8.595	8.35	4.713	3800
13	8.595	8.35	2.170	3187
16	8.595	8.35	1.506	2187
17	8.595	8.35	1.500	2004

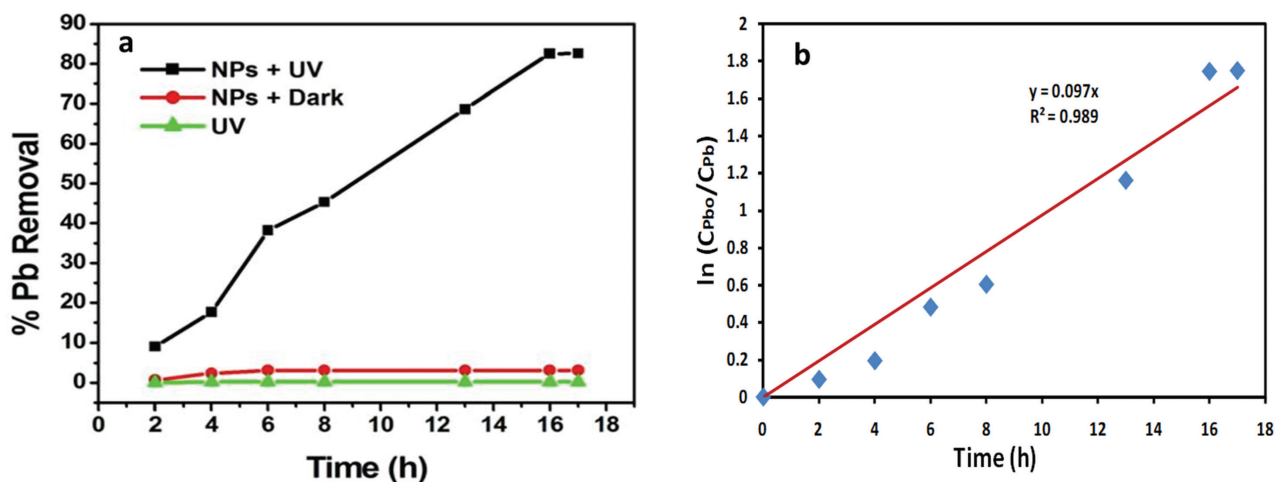


Figure 8: (a) Pb removal profile in UV and dark condition in the presence of synthesized TiO<sub>2</sub> NPs; (b) Kinetic data for Pb removal with synthesized TiO<sub>2</sub> NPs.

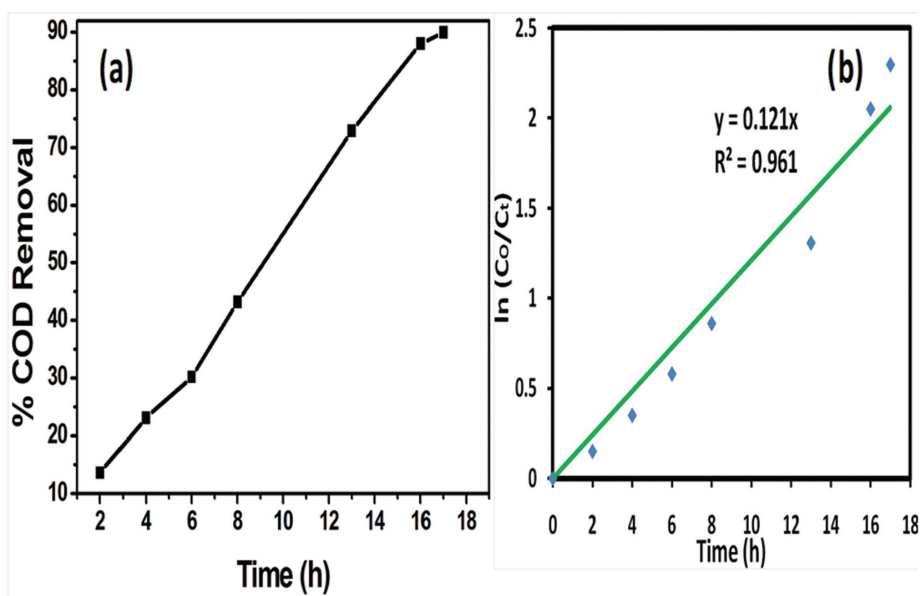


Figure 9: (a) COD removal profile in UV light; (b) Kinetic data for COD removal with the synthesized TiO<sub>2</sub> nanoparticles.

effect to aquatic life [37]. However, a considerable decrease in chemical oxygen demand (COD) was observed after the photo catalytic treatment of wastewater using synthesized nanoparticle i.e. TiO<sub>2</sub> NPs, and 75.5% removal was achieved. The COD removal profile was shown in Figure 9a which was evaluated in the manner similar to lead removal. Kinetic study for COD removal as shown in Figure 9b also shows a good approximation for first-order kinetic with R<sup>2</sup> > 0.95 and rate constant 0.121 h<sup>-1</sup>.

## 4 Conclusion

*Syzygium cumini* leaf extract was used for the synthesis of TiO<sub>2</sub> nanoparticles by a green approach and the obtained nanoparticles were characterized to evaluate physical, chemical, structural and morphological behavior. Present method of synthesis proved to be useful in controlling the size of TiO<sub>2</sub> nanoparticles, thereby tuning their catalytic properties. Synthesized TiO<sub>2</sub> nanoparticles were spherical and aggregated into an irregular structure with an average diameter of 18 nm in size. They possess average crystalline size, surface area, pore size diameter and total pore volume of 10 nm, 105 m<sup>2</sup>/g, 10.50 nm, and 0.278 cm<sup>3</sup>/g, respectively. Synthesized nanoparticles were successfully used as a photo-catalyst for removal of lead from explosive industrial waste water in a cost-effective way with 75.5% removal of chemical oxygen demand (COD) and 82.53% removal of lead (Pb<sup>2+</sup>). Kinetic study reveals that 1<sup>st</sup> order kinetics was followed for photo-catalytic removal of lead as well as the COD removal of the industrial wastewater.

**Acknowledgement:** One of the authors (Naresh Kumar Sethy) would like to thanks ministry of Human Resource Development, from the Department of Chemical Engineering and Technology, IIT (BHU) Varanasi for financial support as SRF. Authors also would like to gratefully acknowledge Sophisticated Lab of Department of Chemical Engineering and Technology and Central Instrument Facility Center (CIFIC), Indian Institute of Technology (BHU), Varanasi for providing instrumental facility, respectively.

## References

- [1] Dhir B., Potential of biological materials for removing heavy metals from wastewater. *Environ. Sci. Pollut. R.*, 2014, 21, 1614-1627.
- [2] Abdel-Halim S.H., Shehata A.M., El-Shahat M.F., Removal of lead ions from industrial waste water by different types of natural materials. *Water Res.*, 2003, 37, 1678-1683.
- [3] Mondal M.K., Removal of Pb (II) ions from aqueous solution using activated tea waste: Adsorption on a fixed-bed column. *J. Environ. Manage.*, 2009, 90, 3266-3271.
- [4] Acharya J., Kumar U., Meikap B., Thermodynamic characterization of adsorption of lead (II) ions on activated carbon developed from tamarind wood from aqueous solution. *S. Afr. J. Chem. Eng.*, 2013, 18, 70-76.
- [5] Singha B., Das S.K., Removal of Pb (II) ions from aqueous solution and industrial effluent using natural biosorbents. *Environ. Sci. Pollut. R.*, 2012, 19, 2212-2226.
- [6] Hu J., Zhao D., Wang X., Removal of Pb(II) and Cu(II) from aqueous solution using multiwalled carbon nanotubes/iron oxide magnetic composites. *Water Sci. Technol.*, 2011, 63, 917-923.
- [7] Dong L., Zhu Z., Qiu Y., Zhao J., Removal of lead from aqueous solution by hydroxyapatite/magnetite composite adsorbent. *Chem. Eng. J.*, 2010, 165, 827-834.
- [8] Halim A.S.H., Shehata A.M.A., Shahat M.F., Removal of lead ions from industrial waste water by different types of natural materials. *Water Res.*, 2003, 37, 1678-1683.
- [9] Goel J., Kadirvelu K., Rajagopal C., Kumar G.V., Removal of lead (II) by adsorption using treated granular activated carbon: batch and column studies. *J. Hazard. Mater.*, 2005, 125, 211-220.
- [10] Uzun H., Bayhana Y.K., Kaya Y., Cakici A., Algur O.F., Biosorption of lead (II) from aqueous solution by cone biomass of *Pinus sylvestris*. *Desalination*, 2003, 154, 233-241.
- [11] Vilar V.J., Botelho C.M., Boaventura R.A., Influence of pH, ionic strength and temperature on lead biosorption by *Gelidium* and agar extraction algal waste. *Process. Biochem.*, 2005, 40, 3267-3275.
- [12] Neppolian B., Choi H.C., Sakthivel S., Arabindoo B., Murugesan V., Solar/UV-induced photocatalytic degradation of three commercial textile dyes. *J. Hazard. Mater.*, 2002, 89, 303-320.
- [13] Sin J.C., Lam S.M., Mohamed A.R., Lee K.T., Degrading endocrine disrupting chemicals from wastewater by TiO<sub>2</sub> photocatalysis: A review. *Int. J. Photoenergy*, 2012, 185159-185182.
- [14] Nakata K., Fujishima A., TiO<sub>2</sub> photocatalysis: Design and applications. *J. Photoch. Photobio. C*, 2012, 13(3), 169-89.
- [15] Lijuan J., Yajun W., Changgen F., Application of photocatalytic technology in environmental safety. *Procedia Engineer.*, 2012, 45, 993-997.
- [16] Chen D., Ray A.K., Removal of toxic metal ions from wastewater by semiconductor photocatalysis. *Chem. Eng. Sci.*, 2001, 56, 1561-1570.
- [17] Devatha C.P., Thalla A.K., Katte S.Y., Green synthesis of iron nanoparticles using different leaf extracts for treatment of domestic waste water. *J. Clean. Prod.*, 2016, 139, 1425-1435.
- [18] Ajitha B., Reddy P.S., Biosynthesis of silver nanoparticles using *Momordica charantia* leaf broth; evaluation of their innate antimicrobial and catalytic activities. *J. Photoch. Photobio. B*, 2015, 146, 1-9.

- [19] Wang T., Jin X., Chen Z., Megharaj M., Naidu R., Green synthesis of Fe nanoparticles using eucalyptus leaf extracts for treatment of eutrophic wastewater. *Sci. Total Environ.*, 2014, 466-467, 210-213.
- [20] Rosi H., Kalyanasundaram S., Synthesis, characterization, structural and optical properties of titanium-dioxide nanoparticles using *Glycosmis cochinchinensis* leaf extract and its photocatalytic evaluation and antimicrobial properties. *WNOFNS*, 2018, 17, 1-15.
- [21] Goutam S.P., Saxena G., Singh V., Yadav A.K., Bharagav R.N., Thapa K.B., Green synthesis of TiO<sub>2</sub> nanoparticles using leaf extract of *Jatropha curcas* L. for photocatalytic degradation of tannery wastewater. *Chem. Eng. J.*, 2018, 336, 386-396.
- [22] Patidar V., Jain P., Green synthesis of TiO<sub>2</sub> nanoparticle using *Moringa oleifera* leaf extract. *Int. Res. J. Eng. Technol.*, 2017, 4, 470-473.
- [23] Rao K.G., Ashok C.H., Rao K.V., Chakra C.S., Tambur P., Green synthesis of TiO<sub>2</sub> nanoparticles using *Aloe vera* extract. *Asian Pac. J. Trop. Med.*, 2015, 2, 28-34.
- [24] Santhoshkumar T., Rahuman A.A., Jayaseelan C., Rajakumar G., Marimuthu S., Kirthi A. V., et al., Green synthesis of titanium dioxide nanoparticles using *Psidium guajava* extract and its antibacterial and antioxidant properties. *Asian Pac. J. Trop. Med.*, 2014, 7, 968-976.
- [25] Muniandy S.S., Kaus N.H.M., Jiang Z.T., Altarawneh M., Lee H.L., Green synthesis of mesoporous anatase TiO<sub>2</sub> nanoparticles and their photocatalytic activities. *RSC Adv.*, 2017, 7, 48083-48094.
- [26] Chen J., Zhang Li., NH<sub>4</sub>Cl-assisted low temperature synthesis of anatase TiO<sub>2</sub> nanostructures from Ti powder. *Mater. Lett.*, 2009, 63, 1797-1799.
- [27] Vadlapudi V., Amanchy R., Phytofabrication of silver nanoparticles using *Myriostachya wightiana* as a novel bioresource, and evaluation of their biological activities. *Braz. Arch. Biol. Technol.*, 2017, 60, DOI:10.1590/1678-4324-2017160329.
- [28] Ghaly Y.M., Jamil S.T., Seesy E.I., Souaya R.E., Nasr A.R., Treatment of highly polluted paper mill wastewater by solar photocatalytic oxidation with synthesized nano TiO<sub>2</sub>. *Chem. Eng. J.*, 2011, 168(1), 446-454.
- [29] Peiro M.A., Peral J., Domingo C., Momenech X., Ayllon A.J., Low-temperature deposition of TiO<sub>2</sub> thin films with photocatalytic activity from colloidal anatase aqueous solutions. *Chem. Mater.*, 2011, 13, 2567-2573.
- [30] Yu J., Su Y., Cheng B., Zhou M., Effects of pH on the microstructures and photocatalytic activity of mesoporous nano crystalline titania powders prepared via hydrothermal method. *J. Mol. Catal. A-Chem.*, 2006, 258, 104-112.
- [31] Martra G., Augugliaro V., Coluccia S., Photocatalytic oxidation of gaseous toluene on polycrystalline TiO<sub>2</sub>: FTIR investigation of surface reactivity of different types of catalysts. *Stud. Surf. Sci. Catal.*, 2000, 130, 665-670.
- [32] Saranya K.S., Padil V.V.T., Senan C., Pilankatta R., Saranya K., George B., et al., Green Synthesis of High Temperature Stable Anatase Titanium Dioxide Nanoparticles Using Gum Kondagogu: Characterization and Solar Driven Photocatalytic Degradation of Organic Dye. *Nanomaterials-Basel*, 2018, 8, 1002-1021.
- [33] Vijayalakshmi R., Rajendran V., Synthesis and characterization of nano-TiO<sub>2</sub> via different methods. *Arch. Appl. Sci. Res.*, 2012, 4(2), 1183-1190.
- [34] Jwo C.S., Tien D.C., Teng T.P., Chang H., Tsung T.T., Liao C.Y., et al., Preparation and UV Characterization of TiO<sub>2</sub> Nanoparticles Synthesized by Sol-gel. *Rev. Adv. Mater. Sci.*, 2005, 10, 283-288.
- [35] Lee S.J., Son H.S., Lee H.K., Zoh K.D., Water Photocatalytic degradation of explosives contaminated water. *Water Sci. Technol.*, 2002, 46(11-12), 139-145.
- [36] Murrini L., Leyva G., Litter M.I., Photocatalytic removal of Pb(II) over TiO<sub>2</sub> and Pt-TiO<sub>2</sub> powders. *Catal. Today*, 2007, 129, 127-135.
- [37] Saxena G., Chandra R., Bharagava R.N., Environmental pollution, toxicity profile and treatment approaches for tannery wastewater and its chemical pollutants. *Rev. Environ. Contam.*, 2016, 240, 31-69.